Pergamon

Int. J. Heat Mass Transfer. Vol. 41, No. 12, pp. 1707–1718, 1998

Printed in Great Britain
0017–9310/98 $19.00+0.00

PII: S0017–9310(97)00266–4

A transient inverse two-dimensional geometry problem in estimating time-dependent irregular boundary configurations

CHENG-HUNG HUANG† and CHIH-CHUNG TSAI

Department of Naval Architecture and Marine Engineering, National Cheng Kung University, Tainan, Taiwan 70101, R.O.C.

(*Received* 8 *April* 1997 *and in final form* 29 *August* 1997)

Abstract—In the present study a transient inverse geometry heat conduction problem (shape identification problem) is solved using the Conjugate Gradient Method (CGM) and Boundary Element Method (BEM)-based inverse algorithm to estimate the unknown irregular boundary shape. Results obtained by using the conjugate gradient method to solve this inverse moving boundary problems are justified based on the numerical experiments. It is concluded that the accurate configuration can be estimated by the conjugate gradient method except for the initial and final time. The reason and improvement of this singularity are addressed. Finally the effects of the measurement errors on the inverse solutions are discussed. © 1998 Elsevier Science Ltd. All rights reserved.

1. INTRODUCTION

The applications of Inverse Heat Conduction Problems (IHCP) can be found in several engineering fields, such as the determination of thermal properties [1], contact resistance [2], etc. Lesnic *et al.* [3] used boundary element method to solve one-dimensional IHCP in estimating boundary thermal behavior. Recently, thermal imaging has become another area of active inverse problem research, and much research has been devoted to infrared scanners and their applications to nondestructive evaluation (NDE) [4–5]. The approaches taken to solve NDE problems are based on either the steady or unsteady state response of a body subjected to thermal sources.

In the previous work by Huang and Chao [6], a steady-state shape identification problem has been solved successfully by using both the Levenberg–Marquardt method [7] and conjugate gradient method [8]. They concluded that the Conjugate Gradient Method (CGM) is better than the Levenberg–Marquardt Method (LMM) since the former needs very short computer time, does not require a very accurate initial guess of the boundary shape and needs fewer sensors. This similar problem has been solved by Hsieh and Kassab [9] and Liu and Zhang [10]. However the techniques they applied are applicable only for the steady-state case.

The objective of the present study is to extend the previous work by Huang and Chao [6] to a transient inverse geometry problem in identifying the unknown irregular boundary configurations from external measurements (either direct or infrared type), based on the boundary element method, i.e. now the boundary shape is a function of time. This makes the entire problem more difficult than the steady-state one since the number of unknowns are increased tremendously. Therefore the Levenberg–Marquardt method holds little promise in solving this kind of identification problem because it is applicable for only parameter estimation problems but now the inverse transient shape identification problem belongs to the function estimation problems. For this reason only the conjugate gradient method is applied here. This approach can be applied to NDE techniques and other problems such as the interface geometry identification for the phase change (Stefan) problems.

The use of Boundary Element Method (BEM) is suggested by the basic nature of the inverse problem (to search an unknown domain, thus an unknown surface), because domain discretization is avoided. More specifically, the advantage gained by BEM-based algorithm is the ability to readily accommodate the changes in the unknown boundary shape as it evolves from its initial to its final shape.

The present work addresses the developments of the conjugate gradient algorithms for estimating unknown boundary shape in transient heat conduction problem. The conjugate gradient method derives from the perturbation principles and transforms the inverse problem to the solution of three problems, namely, the direct, sensitivity and the adjoint problem. The method will be discussed in detail.

† Author to whom correspondence should be addressed.

NOMENCLATURE

c	boundary shape dependent coefficient
$f(x,t)$	unknown irregular boundary configuration
G, H	geometry and time dependent matrix
J	functional defined by equation (6)
J'	gradient of functional defined by equation (15)
k	thermal conductivity
K	thermal diffusivity
M	number of thermocouple
P	direction of descent defined by equation (7b)
q	heat flux density
$T(x,y,t)$	estimated temperature
$Y(x,0,t)$	measured temperature.

Greek symbols

β	search step size
γ	conjugate coefficient
Γ	boundary of the computational domain
$\delta(\cdot)$	Dirac delta function
Δ	perturbed value
$\Delta T(x,y,t)$	sensitivity function defined by equation (8)
ε	convergence criteria
$\lambda(x,y,t)$	Lagrange multiplier defined by equation (13)
σ	standard deviation of the measurement errors
ω	random number
Ω	computational domain.

Superscripts

$\hat{}$	estimated values
n	iteration index
$*$	fundamental solution.

2. THE DIRECT PROBLEM

To illustrate the methodology for developing expressions for use in determining an unknown boundary geometry in a homogeneous medium with thermal diffusivity K, we consider the following two-dimensional inverse moving boundary heat conduction problem. For a domain Ω, the initial temperature equals T_0. When $t > 0$, the boundary conditions at $x = 0$ and L are assumed both insulated, at $y = 0$, a constant cooling heat flux q_0/k is imposed while the boundary condition along boundary $y = f(x,t)$ is a constant temperature T_1. Figure 1 shows the geometry and the coordinates for the two-dimensional physical problem considered here, where the triangles Δ ($M = 20$) and dots $\cdot$ ($M = 10$) denote the sensor locations.

The mathematical formulation of this linear moving boundary heat conduction problem is given by:

$$\frac{\partial^2 T}{\partial x^2} + \frac{\partial^2 T}{\partial y^2} = \frac{1}{K}\frac{\partial T}{\partial t} \quad \text{in } \Omega, \quad t > 0 \tag{1a}$$

$$\frac{\partial T}{\partial x} = 0 \quad \text{at } x = 0, \quad t > 0 \tag{1b}$$

$$\frac{\partial T}{\partial x} = 0 \quad \text{at } x = L, \quad t > 0 \tag{1c}$$

$$\frac{\partial T}{\partial y} = q_0/k \quad \text{at } y = 0, \quad t > 0 \tag{1d}$$

$$T = T_1 \quad \text{at } y = f(x,t), \quad t > 0 \tag{1e}$$

$$T = T_0 \quad \text{at } t = 0, \quad \text{in } \Omega. \tag{1f}$$

The boundary integral equation for this transient problem without a generation term can be derived as [11]

$$cT_N(t_J) + K\int_0^{t_J}\int_\Gamma T_q^* \,\mathrm{d}\Gamma\,\mathrm{d}t = K\int_0^{t_J}\int_\Gamma qT^*\,\mathrm{d}\Gamma\,\mathrm{d}t + \int_\Omega T_0 T^*\,\mathrm{d}\Omega \tag{2}$$

where K is the thermal diffusivity, t_J represents the final time and N denotes a point of Γ or Ω. T^* is now a Green's function that depends on space and time and q^* is its normal derivative given as [11]

$$T^* = \frac{1}{4\pi K\tau}\exp\left[-\frac{r^2}{4K\tau}\right] \tag{3a}$$

$$q^* = \frac{d}{8\pi K^2\tau^2}\exp\left[-\frac{r^2}{4K\tau}\right] \tag{3b}$$

where r is the distance from N to a point of Γ, $\tau = t_J - t$ and d is the distance from a point under consideration to the line along the boundary element.

Let us assume that the initial condition $T_0 = 0$, i.e. the domain integral associated with initial conditions vanishes, and use N constant elements over space domain and J constant elements over time domain. Based on these assumptions, the following discretized boundary integral equation is obtained

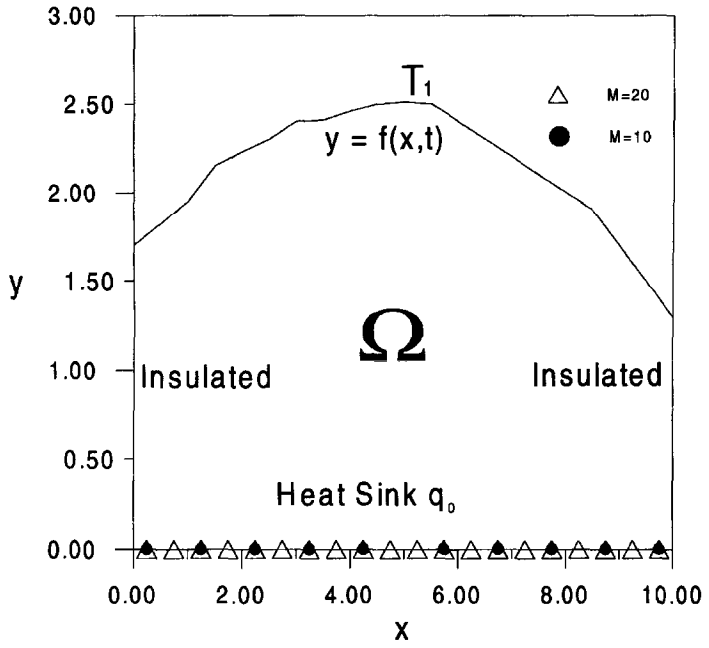

Fig. 1. Geometry and coordinates.

$$\mathbf{C}\mathbf{T}_{,j} + \sum_{j=1}^{J} \mathbf{H}_{jJ}\mathbf{T}_j = \sum_{j=1}^{J} \mathbf{G}_{jJ}\mathbf{Q}_j. \tag{4}$$

Where $\mathbf{T}$ = vector of temperature over N boundary elements at time j, $\mathbf{Q}$ = vector of the heat flux densities at time j, $\mathbf{H}$, $\mathbf{G}$ = geometry and time dependent matrices of dimension (N, N), $\mathbf{C}$ = diagonal matrix of dimension (N, N).

Transferring all unknowns to the left-hand side gives

$$\mathbf{AX} = \mathbf{B} \tag{5}$$

where $\mathbf{X}$ is the vector of unknown T and q boundary values. $\mathbf{B}$ is found by multiplying the corresponding columns by the known values of T's or q's.

The computer program for this transient moving boundary heat conduction problem is modified based on the steady-state potential problem given in the text book by Brebbia and Dominguez [11] and the constant boundary elements over space and time are adopted for all the examples illustrated here.

The direct problem considered here is concerned with the determination of the medium temperature when the moving boundary geometry $f(x, t)$ and the boundary conditions at all boundaries are known.

3. THE INVERSE PROBLEM

For the inverse problem, the boundary geometry along $y = f(x, t)$ is regarded as being unknown, but everything else in equation (1) are known. In addition, temperature readings taken at some appropriate locations and time are considered available.

Referring to Fig. 1, we assumed that M sensors installed along $y = 0$ are used to record the temperature information to identify boundary configuration along $y = f(x, t)$ in the inverse calculations. Let the temperature reading taken within these sensors be denoted by $Y(x_m, 0, t) \equiv Y_m(t)$, $m = 1$ to M, where M represents the number of thermocouples. We note that the measured temperature $Y_m(t)$ contains measurement errors. Then the inverse problem can be stated as follows: by utilizing the above mentioned measured temperature data $Y_m(t)$, estimate the unknown upper boundary shape $f(x, t)$.

The solution of the present inverse problem is to be obtained in such a way that the following functional is minimized:

$$J[f(x,t)] = \int_{t=0}^{t_J} \sum_{m=1}^{M} [T_m(t) - Y_m(t)]^2 \, \mathrm{d}t \tag{6}$$

here, $T_m(t)$ are the estimated or computed temperatures at the measurement locations $(x_m, 0)$ at time t. These quantities are determined from the solution of the direct problem given previously be using an estimated $\hat{f}(x, t)$ for the exact $f(x, t)$. Here the hat '^' denotes estimated quantities.

4. CONJUGATE GRADIENT METHOD FOR MINIMIZATION

The following iterative process based on the conjugate gradient method [8] can be used for the esti-

mation of unknown boundary function $f(x, t)$ by minimizing the functional $J[f(x, t)]$ as:

$$\hat{f}^{n+1}(x, t) = \hat{f}^{n}(x, t) - \beta^{n} P^{n}(x, t) \quad \text{for } n = 0, 1, 2, \ldots \tag{7a}$$

where β^n is the search step size in going from iteration n to iteration $n+1$, and $P^n(x, t)$ is the direction of descent (i.e. search direction) given by

$$P^{n}(x, t) = J'^{n}(x, t) + \gamma^{n} P^{n-1}(x, t) \tag{7b}$$

which is a conjugation of the gradient direction $J'^n(x, t)$ at iteration n and the direction of descent $P^{n-1}(x, t)$ at iteration $n-1$. The conjugate coefficient is defined as

$$\gamma^{n} = \frac{\int_{t=0}^{t_f} \int_{x=0}^{L} (J'^{n})^2 \, \mathrm{d}x \, \mathrm{d}t}{\int_{t=0}^{t_f} \int_{x=0}^{L} (J'^{n-1})^2 \, \mathrm{d}x \, \mathrm{d}t} \quad \text{with } \gamma^{0} = 0. \tag{7c}$$

We note that when $\gamma^n = 0$ for any n, in equation (7b), the direction of descent $P^n(x, t)$ becomes the gradient direction, i.e. the 'Steepest descent' method is obtained. The convergence of the above iterative procedure in minimizing the functional J is guaranteed in [12].

To perform the iterations according to equations (10), we need to compute the step size β^n and the gradient of the functional $J'^n(x, t)$. In order to develop expressions for the determination of these two quantities, a 'sensitivity problem' and an 'adjoint problem' are constructed as described below.

4.1. *Sensitivity problem and search step size*

The sensitivity problem is obtained from the original direct problem defined by equation (1) by assuming that when $f(x, t)$ undergoes a variation $\Delta f(x, t)$, T is perturbed by $T + \Delta T$. Then replacing f in the direct problem by $f + \Delta f$ and T by $T + \Delta T$, subtracting from the resulting expressions the direct problem and neglecting the second-order terms, the following sensitivity problem for the sensitivity function ΔT is obtained.

$$\frac{\partial^2 \Delta T}{\partial x^2} + \frac{\partial^2 \Delta T}{\partial y^2} = \frac{\partial \Delta T}{\partial t} \quad \text{in } \Omega, \quad t > 0 \tag{8a}$$

$$\frac{\partial \Delta T}{\partial x} = 0 \quad \text{at } x = 0, \quad t > 0 \tag{8b}$$

$$\frac{\partial \Delta T}{\partial x} = 0 \quad \text{at } x = L, \quad t > 0 \tag{8c}$$

$$\frac{\partial \Delta T}{\partial y} = 0 \quad \text{at } y = 0, \quad t > 0 \tag{8d}$$

$$\Delta T = \Delta f \frac{\partial T}{\partial y} \quad \text{at } y = f(x, t), \quad t > 0 \tag{8e}$$

$$\Delta T = 0 \quad \text{at } t = 0, \quad \text{in } \Omega \tag{8f}$$

and the BEM technique is used to solve this sensitivity problem.

The functional $J(\hat{f}^{n+1})$ for iteration $n+1$ is obtained by rewriting equation (6) as

$$J(\hat{f}^{n+1}) = \int_{t=0}^{t_f} \sum_{m=1}^{M} [T_m(\hat{f}^{n} - \beta^{n} P^{n}) - Y_m]^2 \, \mathrm{d}t \tag{9a}$$

where we replaced $\hat{f}^{n+1}$ by the expression given by equation (7a). If temperature $T_m(\hat{f}^n - \beta^n P^n)$ is linearized by a Taylor expansion, then equation (9a) takes the form

$$J(\hat{f}^{n+1}) = \int_{t=0}^{t_f} \sum_{m=1}^{M} [T_m(\hat{f}^{n}) - \beta^{n} \Delta T_m(P^{n}) - Y_m]^2 \, \mathrm{d}t \tag{9b}$$

where $T_m(\hat{f}^n)$ is the solution of the direct problem by using the estimate $\hat{f}^n(x, t)$ for exact $f(x, t)$ at $x = x_m$ and time t. The sensitivity function $\Delta T_m(P^n)$ is taken as the solutions of problem (8) at the measured positions $x = x_m$ and time t by letting $\Delta f = -P^n$. The search step size β^n is determined by minimizing the functional given by equation (9b) with respect to β^n. The following expression is obtained:

$$\beta^{n} = \frac{\int_{t=0}^{t_f} \sum_{m=1}^{M} [T_m(t) - Y_m(t)] \Delta T_m(t) \, \mathrm{d}t}{\int_{t=0}^{t_f} \sum_{m=1}^{M} [\Delta T_m(t)^2] \, \mathrm{d}t}. \tag{10}$$

4.2. *Adjoint problem and gradient equation*

To obtain the adjoint problem, equation (1a) is multiplied by the Lagrange multiplier (or adjoint function) $\lambda(x, y, t)$ and the resulting expression is integrated over the corresponding space domains. Then the result is added to the right hand side of equation (6) to yield the following expression for the functional $J[f(x, t)]$ as:

$$J[f(x, t)] = \int_{t=0}^{t_f} \int_{x=0}^{L} [T - Y]^2 \delta(x - x_m) \, \mathrm{d}x \, \mathrm{d}t + \int_{t=0}^{t_f} \int_{x=0}^{L} \int_{y=0}^{f(x,t)} \lambda \left\{ \frac{\partial^2 T}{\partial x^2} + \frac{\partial^2 T}{\partial y^2} - \frac{\partial T}{\partial t} \right\} \mathrm{d}y \, \mathrm{d}x \, \mathrm{d}t. \tag{11}$$

The variation ΔJ is obtained by perturbing f by Δf and T by ΔT in equation (11), subtracting from the resulting expression the original equation (11) and neglecting the second-order terms. This gives:

$$\Delta J = \int_{t=0}^{t_f} \int_{x=0}^{L} 2(T - Y) \Delta T \delta(x - x_m) \, \mathrm{d}x \, \mathrm{d}t + \int_{t=0}^{t_f} \int_{x=0}^{L} \int_{y=0}^{f(x,t)} \lambda \left[\frac{\partial^2 \Delta T}{\partial x^2} + \frac{\partial^2 \Delta T}{\partial y^2} - \frac{\partial \Delta T}{\partial t} \right] \mathrm{d}y \, \mathrm{d}x \, \mathrm{d}t \tag{12}$$

where $\delta(x - x_i)$ is the Dirac delta function and x_m ($m = 1$ to M) refers to the measured positions. In

equation (12), the triple integral term is integrated by parts, the boundary conditions of the sensitivity problem given by equations (8b)–(8e) are utilized and then ΔJ is allowed to go to zero. The vanishing of the integrands containing ΔT leads to the following adjoint problem for the determination of $\lambda(x, y, t)$:

$$\frac{\partial^2 \lambda}{\partial x^2} + \frac{\partial^2 \lambda}{\partial y^2} + \frac{\partial \lambda}{\partial t} = 0 \quad \text{in}\,\Omega, \quad t > 0 \tag{13a}$$

$$\frac{\partial \lambda}{\partial x} = 0 \quad \text{at}\, x = 0, \quad t > 0 \tag{13b}$$

$$\frac{\partial \lambda}{\partial x} = 0 \quad \text{at}\, x = L, \quad t > 0 \tag{13c}$$

$$\frac{\partial \lambda}{\partial y} = -2(T - Y)\delta(x - x_m) \quad \text{at}\, y = 0 \quad t > 0 \tag{13d}$$

$$\lambda = 0 \quad \text{at}\, y = f(x, t), \quad t > 0 \tag{13e}$$

$$\lambda = 0 \quad \text{at}\, t = t_F, \quad \text{in}\,\Omega. \tag{13f}$$

The adjoint problem is different from the standard initial value problem in that the final time condition at time $t = t_J$ is specified instead of the customary initial condition. However, this problem can be transformed to an initial value problem by the transformation of the time variables as $\tau = t_J - t$. Then the standard techniques of BEM can be used to solve the above adjoint problem.

Finally, the following integral term is left

$$\Delta J = \int_{t=0}^{t_J} \int_{x=0}^{L} -\left[\frac{\partial \lambda}{\partial y}\frac{\partial T}{\partial y}\right]_{y=f(x,t)} \Delta f(x, t)\, \mathrm{d}x\, \mathrm{d}t. \tag{14a}$$

From definition [8], the functional increment can be presented as

$$\Delta J = \int_{t=0}^{t} \int_{x=0}^{L} J'(x, t)\Delta f(x, t)\, 2\mathrm{d}x\, \mathrm{d}t. \tag{14b}$$

A comparison of equations (14a) and (14b) leads to the following expression for the gradient of functional $J'(x, t)$ of the functional $J[f(x, t)]$:

$$J'(x, t) = -\left.\frac{\partial \lambda}{\partial y}\frac{\partial T}{\partial y}\right|_{y=f(x,t)}. \tag{15a}$$

We note that $J'(x, t_J)$ and $J'(x, 0)$ are always equal to zero since $[\partial \lambda(x, y, t_J)/\partial y] = 0$ and $[\partial T(x, y, 0)/\partial y] = 0$. If the initial values of $f(x, 0)$ and final time values of $f(x, t_J)$ can not be predicted before the inverse calculation, the estimated values of $f(x, t)$ will deviate from exact values near both initial and final time conditions. This is the case in the present study. However, if we let

$$\frac{\partial T(x, y, 0)}{\partial y} = \frac{\partial T(x, y, \Delta t)}{\partial y} \tag{15b}$$

$$\frac{\partial \lambda(x, y, t_J)}{\partial y} = \frac{\partial \lambda(x, y, t_J - \Delta t)}{\partial t} \tag{15c}$$

where Δt denotes the time increment used in the finite difference calculation. By applying (15b) and (15c) to the gradient equation (15a), the singularity at $t = t_0$ and t_J can be avoided in the present study and reliable inverse solutions can be obtained.

4.3. *Stopping criterion*

If the problem contains no measurement errors, the traditional check condition is specified as

$$J[\hat{f}^{n+1}(x, t)] < \varepsilon \tag{16a}$$

where ε is a small specified number. However, the observed temperature data may contain measurement errors. Therefore, we do not expect the functional equation (6) to be equal to zero at the final iteration step. Following the experience of the author [8], we use the discrepancy principle as the stopping criterion, i.e. we assume that the temperature residuals may be approximated by

$$T_m(t) - Y_m(t) \approx \sigma \tag{16b}$$

where σ is the standard deviation of the measurements, which is assumed to be a constant. Substituting equation (16b) into equation (6), the following expression is obtained for stopping criteria ε:

$$\varepsilon = M\sigma^2 t_J. \tag{16c}$$

5. COMPUTATIONAL PROCEDURE

The computational procedure for the solution of this inverse problem using conjugate gradient method may be summarized as follows:

Suppose $\hat{f}^n(x, t)$ is available at iteration n.

Step 1. Solve the direct problem given by equation (1) for $T(x, y, t)$.

Step 2. Examine the stopping criterion given by equation (16a) with ε given by equation (16c). Continue if not satisfied.

Step 3. Solve the adjoint problem given by equation (13) for $\lambda(x, y, t)$.

Step 4. Compute the gradient of the functional J' from equation (15).

Step 5. Compute the conjugate coefficient γ^n and direction of descent P^n from equations (7c) and (7b), respectively.

Step 6. Set $\Delta f(x, t) = -P^n(x, t)$, and solve the sensitivity problem given by equation (8) for $\Delta T(x, y, t)$.

Step 7. Compute the search step size β^n from equation (10).

Step 8. Compute the new estimation for $\hat{f}^{n+1}(x, t)$ from equation (7a) and return to step 1.

6. RESULTS AND DISCUSSIONS

To illustrate the validity of the present inverse moving boundary algorithm in identifying irregular boundary configuration $f(x, t)$ from the knowledge

of spatial and temporal temperature recordings, we consider two specific examples where the boundary geometry at $y = f(x, t)$ is assumed as a sinusoidal function and a step function, respectively.

The objective is to show the accuracy of the present approach in estimating $f(x, t)$ with no prior information on the functional form of the unknown quantities, which is the so-called function estimation. Moreover, it can be shown numerically that the number of sensors can be reduced when the conjugate gradient method is applied.

In order to compare the results for situations involving random measurement errors, we assume normally distributed uncorrelated errors with zero mean and constant standard deviation. The simulated inexact measurement data $\mathbf{Y}$ can be expressed as

$$\mathbf{Y} = \mathbf{Y}_{\text{exact}} + \omega\sigma \tag{17}$$

where $\mathbf{Y}_{\text{exact}}$ is the solution of the direct problem with an exact $f(x, t)$; σ is the standard deviation of the measurements; and ω is a random variable that was generated by subroutine DRNNOR of the IMSL [13] and will be within -2.576 to 2.576 for a 99% confidence bounds.

In all the test cases considered here, we have chosen $L = 10$, $T_0 = 0$, $T_1 = 100$, $K = 1$, $q_0/k = 100$, $t_J = 18$, $\Delta t = 1$ and 20 constant elements are used on both upper and lower boundaries, while three linear elements are adopted for right and left boundaries. The sensor's locations are always along $y = 0$, i.e. on the lower boundary.

We now present below the numerical experiments in determining $f(x, t)$ by the inverse analysis:

6.1. *Numerical test case* 1

The unknown boundary configuration at $y = f(x, t)$ is assumed to vary with x and t as:

$$y(x, t) = 1.5 - 0.04t + (0.16t)\sin\left(\frac{\pi x}{5}\right);$$
$$0 \leqslant t < 5$$
$$y(x, t) = 1.86 - 0.04t - (0.16t - 1.44)\sin\left(\frac{\pi x}{5}\right);$$
$$5 \leqslant t < 14$$
$$y(x, t) = 2.22 - 0.04t + (0.16t - 2.88)\sin\left(\frac{\pi x}{5}\right);$$
$$14 \leqslant t \leqslant 18 \tag{18}$$

the exact plot for the boundary configuration is shown in Fig. 2.

The inverse analysis is first performed by using 20 thermocouple measurements (referring to Fig. 1 where the triangle $\triangle$ denotes the sensor's location) with thermocouple spacing $\Delta x = 0.5$. When assuming exact measurements ($\sigma = 0.0$), and using *good* initial guess $\mathbf{f}^0 = 1.5$ (the word 'good' means the boundary configurations at initial and final time are the same as the initial guess values) the estimated function of $f(x, t)$ by using the CGM is shown in Fig. 3. It can be seen from Figs. 2 and 3 that the CGM obtained good estimation of $f(x, t)$.

The average relative error between exact and estimated values after 20 iterations is 1.11% for the present case and the average relative error is defined as

$$\text{error \%} = \sum_{i=1}^{I}\sum_{j=0}^{J}\left|\frac{f(x_i, t_j) - \hat{f}(x_i, t_j)}{f(x_i, t_j)}\right| \div [(I) \times (J+1)] \times 100\% \tag{19}$$

here I and $(J+1)$ represents the total discrete number of unknown parameters and time, respectively, while f and $\hat{f}$ denote the exact and estimated values of boundary configuration. This shows that when an accurate initial guess $\mathbf{f}^0$ is provided, the validity of the CGM is thus proved.

Next, let us discuss what will happen when the initial guess $\mathbf{f}^{(0)}$ deviates from the exact solutions at the initial and final time step. The computational situations are the same as before except that the initial guess is now chosen as $\mathbf{f}^0 = 2.0$. The average relative error of the inverse solutions after 20 iterations is 3.89%. It is clear that the estimated $f(x, t)$ is still reliable except for the values near $t = t_0$ and t_J where the estimated values of the boundary shape remains the same as the initial guess values $f(x, t_0) = f(x, t_J) = 2.0$. The reason for this singularity is stated previously and not repeated here.

However, if the artificial gradients at $t = t_0$ and t_J are determined from equations (15b) and (15c), the singularity which occurs at $t = t_0$ and t_J can be improved significantly. The results obtained by using equations (15b) and (15c) at $t = t_0$ and t_J is shown in Fig. 4, the average relative error between exact and estimated values after 20 iterations is now 2.53%. It is evident that the error can be reduced by the application of equations (15b) and (15c).

The above test cases seem unrealistic, since too many sensors were used in the numerical experiments. Now the question arises, can the number of sensors be reduced with the present approach? Let us first take a look at the role of measured temperature played in CGM. The measurement temperatures at sensor locations represent a boundary point heat flux that appeared in the adjoint equations (13). Therefore it is possible to reduce the number of boundary point heat fluxes even though it will influence the value of J'. Now the question is that will this strategy influence the accuracy of the inverse solutions? To answer this, the numerical experiment is proceeded to the next case by utilizing $\mathbf{f}^0 = 2.0$ and $M = 10$ (as was shown in Fig. 1), in estimating $f(x, t)$ with measurement error $\sigma = 0.0$. The inverse solutions in predicting $f(x, t)$ under such an assumption using the CGM is shown in Fig. 5. The average relative error between exact and estimated values after 20 iterations is 3.55%.

From the comparison of numerical data in Figs. 4 and 5, it is seen that the inverse solutions in predicting

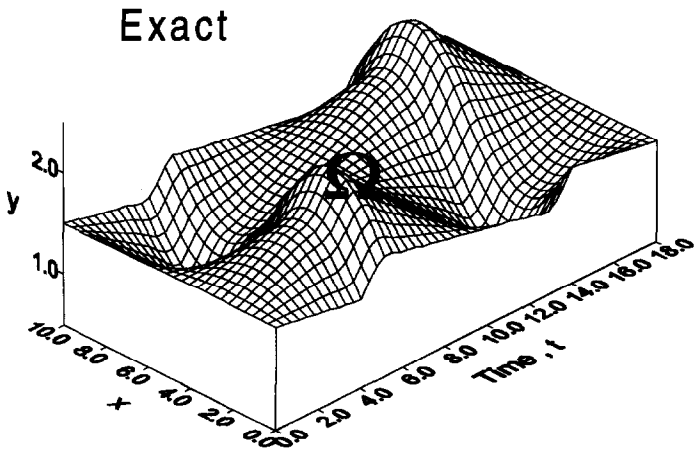

Fig. 2. Exact plot for the moving boundary configurations $f(x, t)$ for case 1.

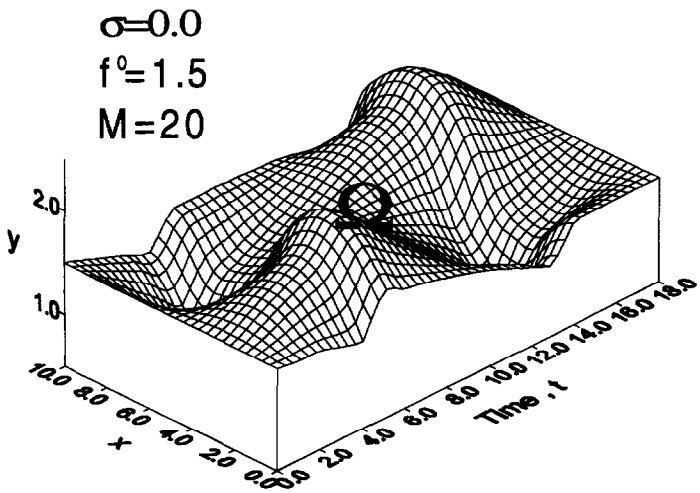

Fig. 3. Inverse solution of $f(x, t)$ by using $\mathbf{f}^0 = 1.5$, $\sigma = 0.0$ and $M = 20$.

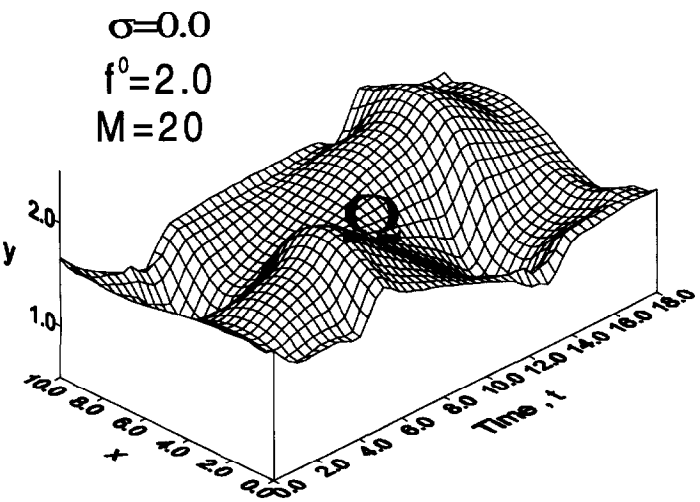

Fig. 4. Inverse solution of $f(x, t)$ by using $\mathbf{f}^0 = 2.0$, $\sigma = 0.0$, $M = 20$ and artificial gradient at $t = t_0$ and t_F.

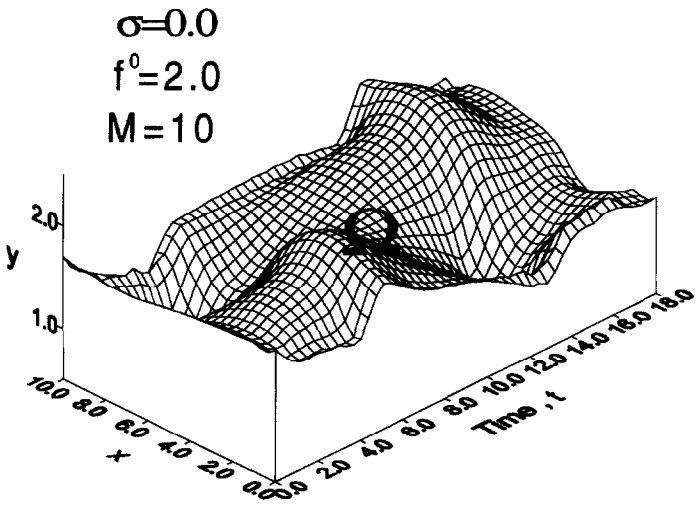

Fig. 5. Inverse solution of $f(x, t)$ by using $\mathbf{f}^0 = 2.0$, $\sigma = 0.0$, $M = 10$ and artificial gradient at $t = t_0$ and t_F.

$f(x, t)$ with 20 sensors are slightly better than that with 10 sensors. However, the latter case is already good enough to be accepted as the inverse solution. Thus the number of sensors can be reduced when the CGM is applied. The following examples use $M = 10$ and the artificial gradients at $t = t_0$ and t_J.

The above numerical experiments were concerned with exact measurements, however measurement errors will always be introduced in any real measurement. It is important to detect the influence of the measurement errors to the inverse solutions under the present algorithm.

Two different noises are introduced here. For the first one we assumed that the error in the order of about 3% maximum measured temperature is introduced according to equation (17), i.e. the dimensionless measured temperatures with errors $\sigma = 3.0$ are considered (since the absolute maximum measured temperature is about 100). Next, measurement error with $\sigma = 5.0$ is used. The inverse solutions using these inexact measurements as the simulated temperature measurements are shown in Figs. 6 and 7.

By using these 3 and 5% errors, the resultant average error of the inverse solutions is about 4.53 and 5.26%, respectively. This implies that the CGM is not sensitive to the measurement errors since the measurement errors did not amplify the errors of estimated boundary shape (the errors are of same order of magnitude). Therefore the present technique provides a good estimation.

In order to show the estimated inverse solutions more clearly, Fig. 8 shows the estimated $f(x, t)$ obtained from Figs. 3 and 7 at time $t = 4$ and 12, respectively.

6.2. *Numerical test case* 2

The unknown boundary configuration at $y = f(x, t)$ is assumed to vary with x and t as:

$$
\begin{aligned}
&y = 1.5+0.2t; \quad 0 \leqslant x < t; \quad 0 \leqslant t < 6\\
&y = 1.5-0.05t; \quad t \leqslant x \leqslant 10; \quad 0 \leqslant t < 6\\
&y = 3.5-0.2t; \quad 0 \leqslant x < t; \quad 6 \leqslant t < 11\\
&y = 1.0+0.05t; \quad t \leqslant x \leqslant 10; \quad 6 \leqslant t < 11\\
&y = 1.5-0.05(t-10); \quad 0 \leqslant x < 10-1.25(t-10);\\
&\qquad 11 \leqslant t < 15\\
&y = 1.5+0.1(t-10); \quad 10-1.25(t-10) \leqslant x \leqslant 10;\\
&\qquad 11 \leqslant t < 15\\
&y = 1.1+0.05(t-10); \quad 0 \leqslant < 10-1.25(t-10);\\
&\qquad 15 \leqslant t \leqslant 18\\
&y = 2.3-0.1(t-10); \quad 10-1.25(t-10) \leqslant x \leqslant 10;\\
&\qquad 15 \leqslant t \leqslant 18
\end{aligned}
\tag{20}
$$

and the exact plot for the boundary configuration is shown in Fig. 9.

The inverse analysis is first performed by using 20 thermocouple measurements. With $\sigma = 0.0$ and using *good* initial guess $\mathbf{f}^0 = 1.5$, the estimated function of $f(x, t)$ is shown in Fig. 10. The average relative error between exact and estimated values after 20 iterations is 2.25% for the present case. It can be seen from Figs. 9 and 10 that the CGM obtained good estimation of $f(x, t)$.

Next we assumed that the error in the order of about 3% maximum measured temperature is introduced according to equation (17), i.e. the dimensionless measured temperatures with errors $\sigma = 3.0$ are considered (since the absolute maximum measured temperature is about 100). The inverse solution using this inexact measurement as the simulated temperature measurements is shown in Fig. 11.

By using this 3% error, the resultant average error of the inverse solution is about 4.73%. In order to show the estimated inverse solutions more clearly, we

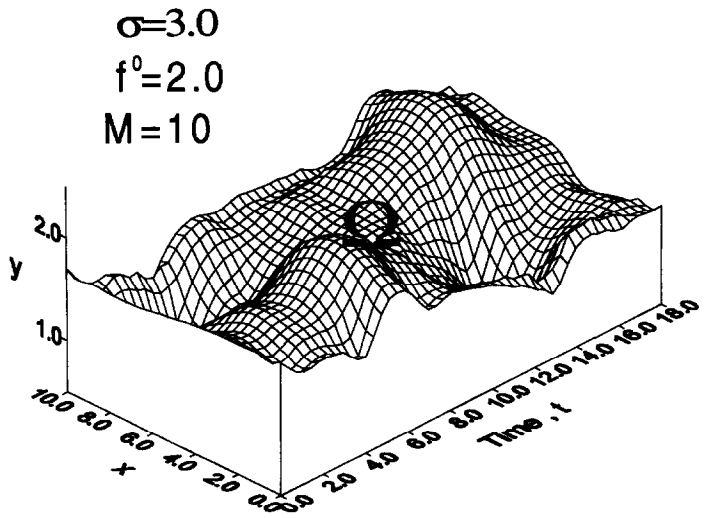

Fig. 6. Inverse solution of $f(x, t)$ by using $\mathbf{f}^0 = 2.0$, $\sigma = 3.0$, $M = 10$ and artificial gradient at $t = t_0$ and t_F.

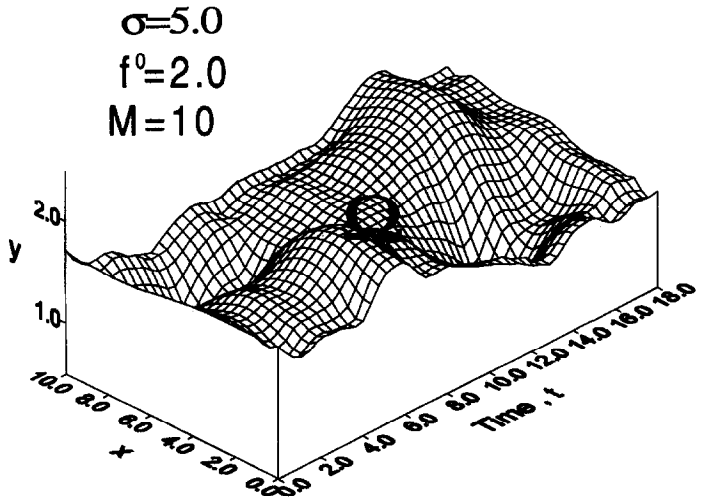

Fig. 7. Inverse solution of $f(x, t)$ by using $\mathbf{f}^0 = 2.0$, $\sigma = 5.0$, $M = 10$ and artificial gradient at $t = t_0$ and t_F.

plot Fig. 12 which is the estimated $f(x, t)$ obtained from Figs. 10 and 11 at time $t = 5$ and 14, respectively.

From above numerical test cases for the present transient inverse geometry problem it is concluded that the advantages of using the CGM in estimating unknown boundary configurations are: (i) the inverse solutions does not exhibit stability (regularity) loss when increasing the measurement errors and (ii) the number of sensor can be reduced without appreciably affecting to accuracy of the accurate inverse solutions.

7. CONCLUSIONS

The Conjugate Gradient Method (CGM) along with the Boundary Element Method (BEM) was successfully applied for the solution of the inverse moving boundary problem to determine the unknown transient irregular boundary configuration by utilizing temperature readings. Several test cases involving different measurement errors were considered. The results show that the inverse solution obtained by CGM remain stable and regular as the measurement errors are increased and the number of sensors can be reduced while accurate boundary shapes can still be obtained when performing the inverse calculations.

Acknowledgement—This work was supported in part through the National Science Council, R.O.C., Grant number, NSC-87-2212-E-006-107.

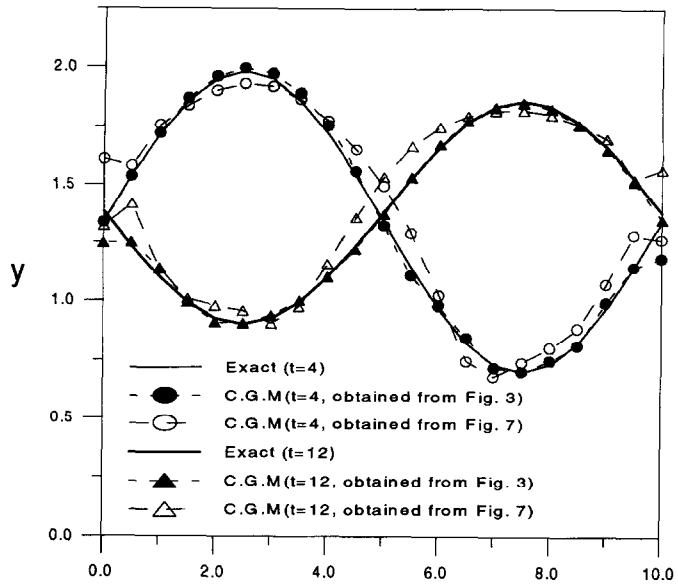

Fig. 8. Comparison of exact and inverse solutions of $f(x, t)$ at $t = 4$ and 12 by extracting data from Figs. 3 and 7.

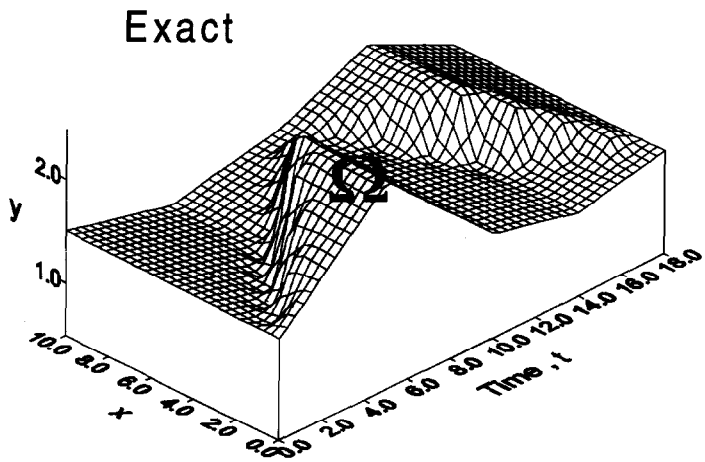

Fig. 9. Exact plot for the moving boundary configurations $f(x, t)$ for case 2.

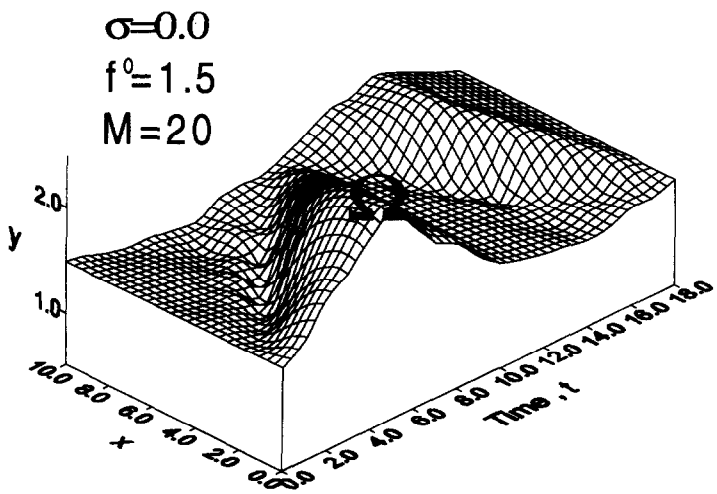

Fig. 10. Inverse solution of $f(x, t)$ by using $\mathbf{f}^0 = 1.5$, $\sigma = 0.0$ and $M = 20$.

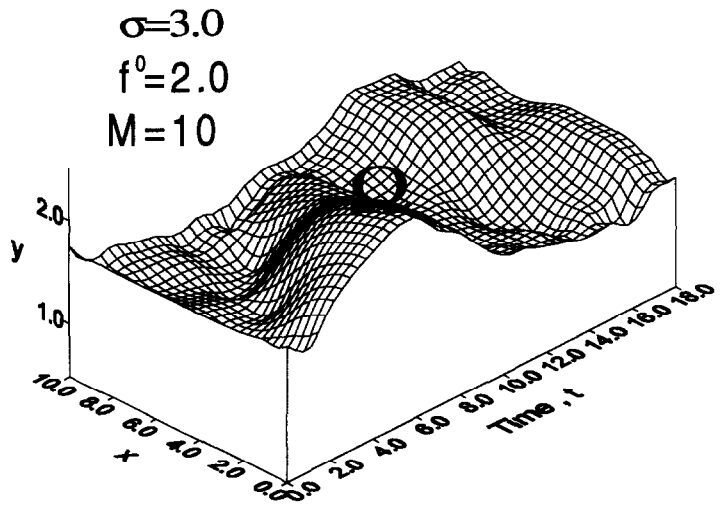

Fig. 11. Inverse solution of $f(x, t)$ by using $f^0 = 2.0$, $\sigma = 3.0$, $M = 10$ and artificial gradient at $t = t_0$ and t_F.

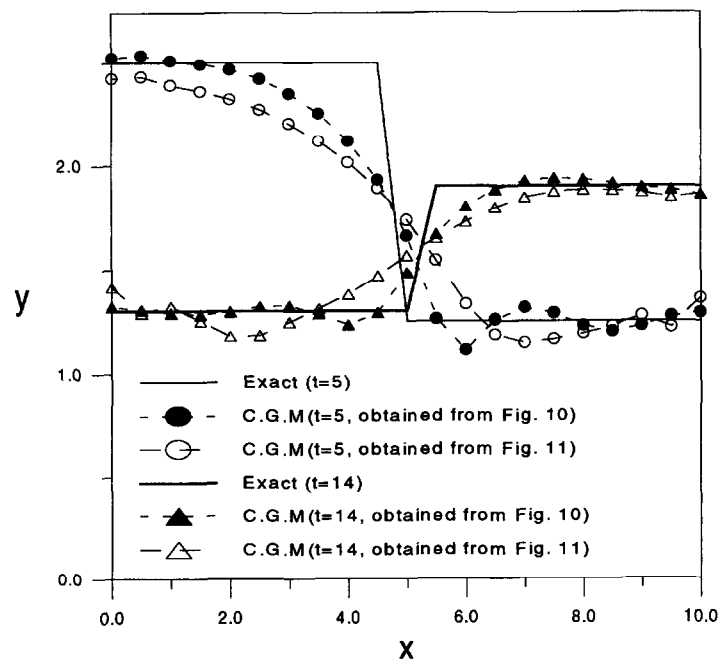

Fig. 12. Comparison of exact and inverse solutions of $f(x, t)$ at $t = 5$ and 14 by extracting data from Figs. 10 and 11.

REFERENCES

1. Huang, C. H. and Yan, J. Y., An inverse problem in simultneously measuring temperature dependent thermal conductivity and heat capacity. *International Journal of Heat and Mass Transfer*, 1995, **38,** 3433–3441.
2. Huang, C. H., Ozisik, M. N. and Sawaf, B., Conjugate gradient method for determining unknown contact conductance during metal casting. *International Journal of Heat and Mass Transfer*, 1992, **35,** 1779–1786.
3. Lesnic, D., Elliott, L. and Ingham, D. B., Application of the boundary element method to inverse heat conduction problems. *International Journal of Heat and Mass Transfer*, 1996, **39,** 1503–1517.
4. Hsieh, C. K. and Su, K. C., A methodology of predicting cavity geometry based on the scanned surface temperature data-prescribed surface temperature at the cavity side. *Journal of Heat Transfer*, 1980, **102,** 324–329.
5. Kassab, A. J. and Pollard, J., A cubic spline anchored grid pattern algorithm for high resolution detection of subsurface cavities by the IR-CAT method. *Num. Heat Transfer, Part B*, 1994, **26,** 63–78.
6. Huang, C. H. and Chao, B. H., An inverse geometry problem in identifying irregular boundary configurations. *International Journal of Heat and Mass Transfer*, 1997, **40,** 2045–2053.
7. Marquardt, D. M., An algorithm for least-squares estimation of nonlinear parameters. *J. Soc. Indust. Appl. Math.*, 1963, **11,** 431–441.
8. Alifanov, O. M., Solution of an inverse problem of heat conduction by iteration methods *Journal of Engineering Physics*, 1972, **26,** 471–476.
9. Hsieh, C. K. and Kassab, A. J., A general method for the solution of inverse heat conduction problem with partially unknown system geomctrics. *International Journal of Heat and Mass Transfer*, 1986, **29,** 47–58.
10. Liu, G. L. and Zhang, D. F., Numerical method for solving inverse problem of heat conduction with unknown boundary based on variational principles with variable domain. *Numerical Methods in Thermal Problems*, ed. R. W. Lewis *et al.* Pineridge Press Limited, London, 1987, 284–295.
11. Brebbia, C. A. and Dominguez, J., *Boundary Elements, An Introductory Course*. McGraw-Hill, New York, 1989.
12. Lasdon, L. S., Mitter, S. K. and Warren, A. D., The conjugate gradient method for optimal control problem. *IEEE Transactions on Automatic Control*, 1967, AC-**12,** 132–138.
13. IMSL Library Edition 10.0. User's Manual: Math Library Version 1.0, IMSL, Houston, TX, 1987.